Aerodynamic Characteristics for a Slender Missile with Wrap-Around Fins

Umberto Catani*
BPD Difesa Spazio, Colleferro, Italy

John J. Bertin†
The University of Texas at Austin, Austin, Texas

Roberto De Amicis‡ and Sergio Masullo§
BPD Difesa Spazio, Colleferro, Italy
and
Stanley A. Bouslog¶
The University of Texas at Austin, Austin, Texas

The aerodynamic coefficients for a slender missile with wrap-around fins have been measured over a Mach number range from 0.3 to 3.03 in a wind-tunnel test program. The configuration variables included the fin geometry, the nose configuration, and the afterbody geometry. The data from the wind-tunnel tests, supplemented by data from a water-table flow simulation and by flight-test measurements indicate the cavity housing had a significant effect on the drag force acting on the rocket. The cavity configuration was modified between flight-test programs in order to produce an "open" cavity for the flow in this region. The increased range observed during the flight tests indicated that substantial reductions in the aerodynamic drag were achieved through the cavity modification.

Nomenclature

$C_{D_{cav}}$ = coefficient for incremental drag force due to presence of a cavity
C_{D_0} = drag coefficient at zero lift (without the base drag contribution)
C_{M_α} = pitching moment coefficient derivative with respect to α
C_N = normal force coefficient
C_{N_α} = normal force coefficent derivative with respect to α
d = (external) diameter of the missile
d_i = diameter of the cavity floor
H = height (or depth) of the cavity
L = length of the cavity
M_∞ = freestream Mach number
p_F = static pressure on the forward-facing step
p_L = static pressure on the leeward-facing step
p_∞ = freestream static pressure
x_{cg} = axial location of the center of gravity
x_{cp} = axial location of the center of pressure
α = angle of attack
γ = specific heat ratio

Introduction

A SATURATION field-rocket system using a self-propelled multitube launcher has recently been designed and developed. The system's ammunition is a free rocket with a caliber of 122 mm boosted by a double-base solid-propellant motor. Several warhead models, different operational purposes, and different external geometries and weights have been developed based on the results of the system's analysis. The rocket's nominal maximum range is 25 km. For the rocket's aerodynamic stabilization during flight, a wrap-around fin configuration has been chosen because of its simplicity and reliability. Such fins can be retracted when the rocket is in the launch tube and are deployed after clearing the tube to provide aerodynamic control. When a first rocket configuration already had been flown successfully, alterations in the system requirements were imposed to increase both the rocket and the motor length. A concurrent redesign of the fins was necessary to maintain the stability of the rocket in flight. For tube-launched rockets that use wrap-around fins, the designer is faced with the need for increased fin area while constrained by a limit on the fin span. The designers had to conduct trade studies involving the chord length, the planform, and the location of the fins. Moreover, changes in the fin design require corresponding changes in the design of the cavity in which the wrap-around fins are housed while the rocket is in the launch tube.

Numerous experimental investigations[1-8] have been conducted to determine the aerodynamic characteristic of slender missiles with wrap-around fins. Although some of the studies included configurations that had a rearward-facing step (formed by concentric cylinders of different diameter)[3,5,6] and another had a boattail configuration,[8] information about the effect of a cavity housing on the aerodynamic coefficients was lacking.

Data from wind-tunnel tests, water-table tests, and flight tests are presented in this paper. These data are compared with computed solutions using a state-of-the-art design code. The aerodynamic coefficients for a slender missile with wrap-around fins were measured over a Mach number range from 0.3 to 3.03 at the National Lucht- en Ruimtevaart Laboratorium in Amsterdam. The configuration variables included in the fin geometry, the nose configuration, and the

Presented as Paper 82-0319 at the AIAA 20th Aerospace Sciences Meeting, Orlando, Fla., Jan. 11-14, 1982; submitted Jan. 22, 1982; revision received June 21, 1982.

*Chief, Flight Mechanics Group.
†Bettie Margaret Smith Professor of Engineering, Department of Aerospace Engineering and Engineering Mechanics. Associate Fellow AIAA.
‡Chief, Fluid Dynamics Group.
§Aerodynamics Specialist.
¶Research Assistant, Department of Aerospace Engineering and Engineering Mechanics. Member AIAA.

afterbody geometry. Since the geometry of the cavity housing the wrap-around fins has an important effect on the drag, the cavity geometry also was a parameter of the flight-test program. The cavity configuration was modified between flight-test programs in order to produce both an "open" cavity as well as a "closed" cavity for the flow in this region. The profile of the cavity had been defined through the water-table flow simulation. The increased range observed during the flight tests indicated that substantial reductions in the aerodynamic drag were achieved through the cavity modification.

Experimental Program

The experimental program included wind-tunnel tests, water-table tests, and flight tests. A brief description of each of these tests follows.

Wind-Tunnel Tests

Aerodynamic coefficients were obtained over a Mach number range from 0.3 to 3.03 in a wind-tunnel test program conducted at the National Lucht- en Ruimtevaart Laboratorium in the Netherlands. The Reynolds number varied from 0.67×10^6 to 3.28×10^6. The configuration variables included the fin geometry, the nose configuration, and the afterbody geometry.

Facilities

The test program made use both of the Transonic Wind Tunnel (HST) and the Supersonic Wind Tunnel (SST). The HST is a variable-density closed-circuit wind tunnel having a test section that is 1.6×2.0 m and a speed range up to Mach 1.37. The Reynolds number can be varied by changing the stagnation pressure from 12 up to 390 kPa. The SST is a blow-down wind tunnel having a test section that is 1.2×1.2 m. The two-dimensional, flexible plate nozzle can be set at discrete positions to provide a range of Mach number. The settling chamber pressure can be chosen between 12 to 1470 kPa, depending on the desired Mach-number/Reynolds-number test condition.

Models

The wind-tunnel models of interest to this paper were one-half scale models of the 122-mm field rocket. As noted, the configuration variables included: the afterbody geometry (AB), the nose geometry (N), and the fin geometry (F). The configurations for which data are presented in this report are as follows.

1) The afterbody geometry: data were obtained on a finless missile both with and without a cavity. The smooth afterbody, i.e., the configuration not having a cavity, is designated AB_2. AB_1 designates the afterbody configuration having a cavity. A detailed sketch of the cavity is included in Fig. 1. All of the finned models had the cavity. For purposes of analysis, the length-to-depth ratio of the cavity was assumed to be 6.

2) The nose geometry: N_1 designates the nose geometry that was used in the body only (i.e., the finless configuration) tests. N_1 was 2.93-calibers long. N_2 designates the nose geometry that was used for the finned missiles. A sketch of the N_2 nose, which was 3.82-calibers long, is presented in Fig. 1.

3) The fin geometry: data are presented for only two of the fins in this paper, a rectangular fin (F_2) and a trapezoidal fin (F_3). Both fins have the same root chord and span. The leading edge of the trapezoidal fin is swept 30 deg. A sketch of a complete configuration, the $AB_1N_2F_2$, is presented in Fig. 1. A photograph of the model in the wind tunnel is presented as Fig. 2. For more information about the wind-tunnel tests, the reader is referred to Ref. 9.

Water-Table Tests

When the length and configuration of the cavity housing were changed to accommodate the longer fins, used with the longer motor, increased drag was observed because the cavity was closed. An investigation of the effect of the cavity geometry on the local flow pattern was conducted using a water table at the Laboratorio di Fluidodinamica at Colleferro. Sketches of the three cavity geometries for which data are presented in this paper appear in Fig. 3. The geometries represent Fig. 3a the short cavity associated with the original motor/fin design, Fig. 3b the long, sloping cavity associated with the initial fin redesign for the lengthened motor, and Fig. 3c the "improved," long-cavity design, intended to provide open cavity flow with the lengthened motor. For additional information about the water-table tests, the reader is referred to Ref. 10.

Flight Tests

Several flight-test programs have been conducted at a range in Sardinia. The rockets have been launched one at a time and in the ripple mode. The configuration variables include the nose geometry, the motor length, the propellant weight, the fin geometry, and the cavity configuraion. Sketches of representative rocket configurations from the flight-test program are presented in Fig. 4. The configurations are in Fig. 4a a short-motor, short-nozzle configuration with the original cavity and small trapezoidal fins; Fig. 4b a long motor, long-nozzle configuration with the long, sloping cavity and rectangular fins; and Fig. 4c a long-motor, long-nozzle configuration with the "improved," long-cavity design and

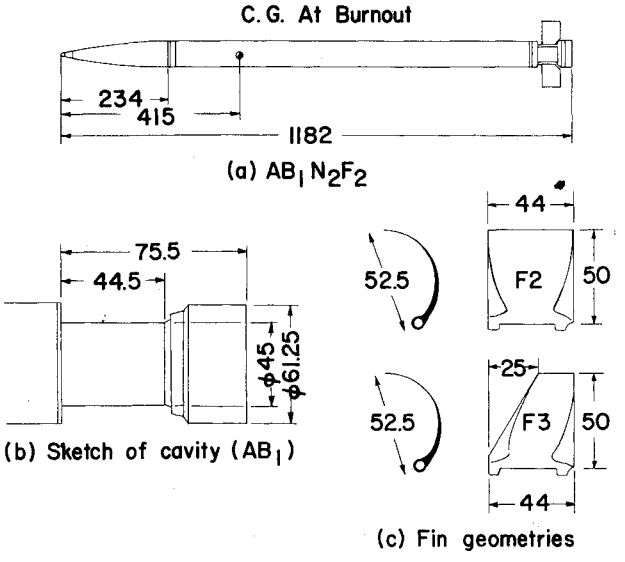

Fig. 1 Sketches of wind-tunnel models (dimensions in millimeters); a) $AB_1N_2F_2$, b) sketch of cavity (AB_1), and c) fin geometries.

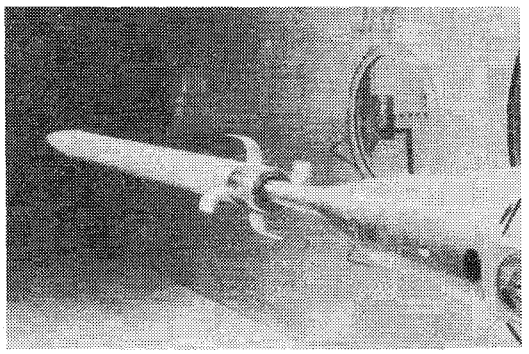

Fig. 2 Photograph of wrap-around fin model in the wind tunnel.

rectangular fins. The root chord of the fins for configurations b and c was 110 mm, while that for configuration a was 88 mm. The ten trajectories presented in this paper are for the same warhead (weight and geometry).

Computed Aerodynamics

A numerical code has been written for the Cyber 175 computer to compute the aerodynamic coefficients based on state-of-the-art engineering correlations. The basic code followed closely that described in Refs. 11 and 12. Thus, for the body alone, the nose wave drag and the boattail wave drag are computed for supersonic flow using second-order van Dyke relations. The inviscid lift, the pitching moment, and the wave drag of the wing-, the tail- and/or the canard-surfaces are computed using linear theory. Wing/body interference and most of the dynamic coefficients are based on empirical correlations. The skin-friction drag (both for the body and for the wing/canard surfaces) is based on the van Driest relations. The "base drag" for the body and for the trailing-edge separation from the wings is based on empirical information. The original code is well documented.[11,12] The reader is referred to these references for more information about the correlations used.

There are significant differences between the present code and that described in Refs. 11 and 12. Several of them relate to the curve-fit procedures and numerical techniques and will not be described here. Two changes worth noting are 1) changes to the empirical input to the transonic wave drag on the nose and 2) the addition of a subroutine to calculate the incremental drag due to the presence of a cavity.

The original empirical input for the axial force coefficient due to the transonic wave drag on the nose were replaced by experimental values taken from the literature.[13,14]

The incremental drag due to the presence of a cavity is calculated assuming that the axial cross section of the cavity is rectangular. The incremental drag is calculated using the relation

$$C_{D_{cav}} = \frac{2}{\gamma M_\infty^2}\left[\left(\frac{p_F}{p_\infty} - \frac{p_L}{p_\infty}\right)\left(1 - \frac{d_i^2}{d^2}\right)\right]$$

Experimental values taken from the literature[15,16] were used to develop tabular correlations for the pressure on the downstream-facing step (p_L/p_∞) and that on the forward-facing (recompression) step (p_F/p_∞).

The trajectories were computed using a six degree-of-freedom code, described in Ref. 17.

Discussion of Results

An extensive experimental investigation of the aerodynamic performance of a 122-mm rocket system has been conducted using the results from wind-tunnel tests, from water-table tests, and from flight tests. The data from these programs have been analyzed using state-of-the-art computer codes.

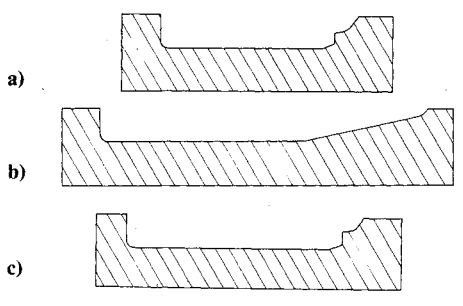

Fig. 3 Sketches of cavity geometries for water-table tests: a) short ...y (original design), b) long, sloping cavity (closed flow), and c) ...oved" long cavity design.

Flowfield Based on Model Tests

Effect of the Cavity

As noted in the Introduction, increased thrust requirements were achieved by increasing the motor length. In the corresponding design modifications, the root chord of the wrap-around fins and the length of the cavity in which they were housed were increased. As a result, the flow in the fin-housing cavity evidently was closed, as indictated by the reduced range obtained during the flight tests. Data from the wind-tunnel tests and from the water-table tests indicate that the cavity-induced drag can represent a considerable contribution to the total drag force on the missile.

Zero angle-of-attack drag coefficients for a finless missile both with (AB_1N_1) and without a cavity (AB_2N_1) are presented in Fig. 5. As noted in the Nomenclature, the base-drag component has been subtracted from the drag coefficients. Recall that AB_1 denotes the afterbody geometry that contains the cavity. Wind-tunnel values of C_{D_0} are presented over a Mach number range from 0.3 to 1.35. The experimentally determined values of C_{D_0} are compared with the computed values. The correlation between the experimental values and the computed values is considered good, except

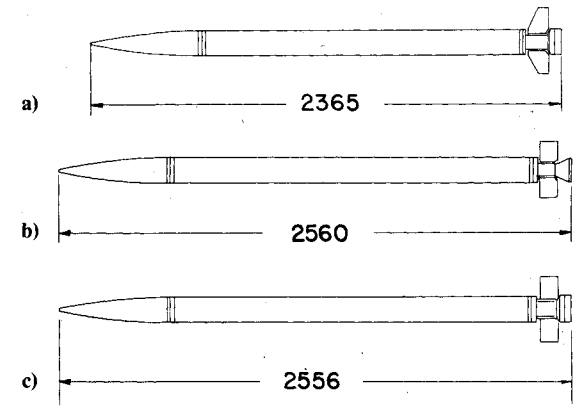

Fig. 4 Sketches of rocket configurations (dimensions in millimeters): a) configuration A, b) configuration B, and c) configuration C.

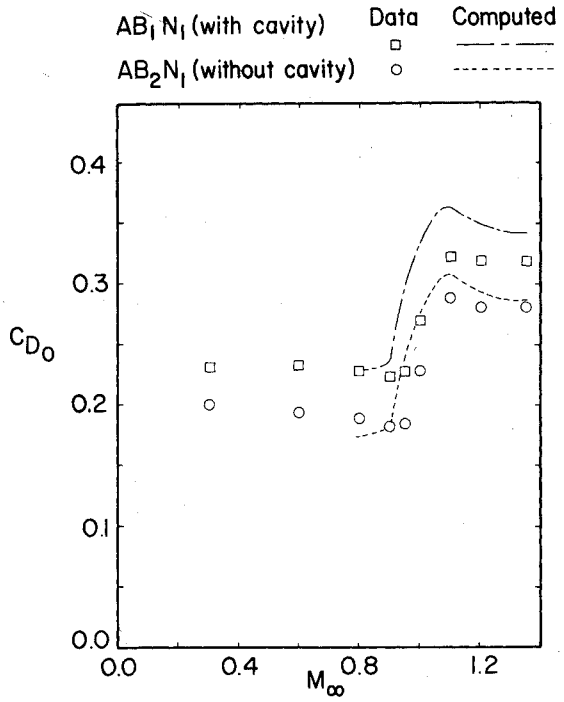

Fig. 5 The effect of the cavity on the zero angle-of-attack drag coefficient for a finless missile.

when the freestream Mach number is very near one. A principal contributor to the differences between the computed drag coefficients and those measured at sonic speeds is attributed to differences between the empirical correlations for the forebody pressure drag used in the computer code and the actual values. Recall (as was noted in the section on Computed Aerodynamics) that the empirical data used to compute the forebody wave drag at transonic speeds was improved.[13,14] Nevertheless, there still exists a need for better correlations at sonic speeds.

The differences between the drag measurements for the two configurations indicate that the cavity-induced drag was essentially constant (at a value of 0.04) for Mach numbers from 0.6 to 1.35. Although the computed value for the cavity-induced increment to the drag coefficient (i.e., 0.054) is slightly greater than the experimental value, the results from the literature[15] used in the cavity-related correlations clearly indicate that the cavity is open for these conditions. That the cavity flow is open is verified by the schlieren photograph from the wind-tunnel tests that is presented in Fig. 6. Note that the flow clearly passes over the cavity. There are, however, two weak shock waves in the cavity region. The one upstream of the cavity is caused by the presence of a slight ramp (see the sketch in Fig. 1). The second is the recompression shock wave at the forward-facing surface of the cavity.

Even though the cavity is relatively short (i.e., $L \simeq 6H$), the cavity-induced drag is a significant fraction of the total drag. Thus, a cavity that would be sufficiently long so that the flow in the cavity is closed would produce even more drag and, therefore, have a significant effect on the range. To determine the appropriate geometry for the missile fin housing, cavity flows were studied using water-table simulations. Three cavity geometries were tested: a) a short cavity ($L \simeq 6H$), similar to that of the wind-tunnel model; b) a long, sloping cavity, similar to that of the flight configuration which exhibited reduced range; and c) the modified design ($L \simeq 7.2H$), which is used on the redesigned missile.

Photographs of the water-table simulations of the cavity flow for a Mach number of 2 are presented in Fig. 7. Note that the cavity is open both for cavity a and for cavity c. This is consistent with wind-tunnel measurements reported by Charwat et al.[15] Charwat et al. observed that the length-to-depth ratio of the cavity should be greater than ten in order for the cavity to be closed. Note also that a "shock wave" is evident at the recompression face for these two cavities. The cavity flow is closed for the long cavity with the gradually sloping recompression surface, i.e., cavity b, as indicated by the water-table simulation of Fig. 7b. Thus, the photographs of Fig. 7 indicate that the water-table flows are similar to those obtained in the wind tunnel.

Using the normalized height of the free surface of the water as a measure of the local pressure, one finds that the pressure variation in the two open cavities is relatively small. The pressure is slightly greater at the recompression surface. However, large pressure variations occur in the long, sloping cavity. The pressure is very low at the rearward-facing step as well as slightly greater on the recompression surface. Thus, the water-table "pressures" are also consistent with the data from other phases of the test program, since the missile with the long, sloping cavity exhibited reduced range in the flight tests.

Aerodynamics of the Missiles with Fins

The zero angle-of-attack drag coefficients for a missile with rectangular fins ($AB_1N_2F_2$) and for one with trapezoidal fins ($AB_1N_2F_3$) are presented in Fig. 8. Wind-tunnel data are presented for Mach numbers from 0.3 to 3.03. Also included in this figure are computed values for the drag coefficients. As indicated in the legend, the computed values for C_{D_0} for the missile with trapezoidal fins represent three variations for the flow model. The solid line represents the basic flow model and includes contributions to the drag due to the forebody pressure, the body skin-friction, and fin-related contributions due to wave drag, skin-friction drag, and fin-separation drag. For the basic flow model, the fin-related drag components are based on the projected planform of the fins. However, because wrap-around fins are a circular-arc surface, they present a greater frontal area and surface area to the oncoming flow. Thus, Dahlke[6] suggests that the calculations of the fin-related drag should be increased by the ratio of the frontal-fin area to the projected-fin area. Thus, the values of C_{D_0} computed using the frontal-fin area are also presented in Fig. 8. The third set of computations (as indicated by the dotted line) includes the cavity drag. It should be noted that the cavity drag calculations do not account for the effect of the fin mountings on the flow in the cavity. The correlation between the measured values of C_{D_0} for $AB_1N_2F_3$ and the computed values is considered very good.

Computed values of C_{D_0} for the basic flow model are also presented for the wind-tunnel configuration with rectangular

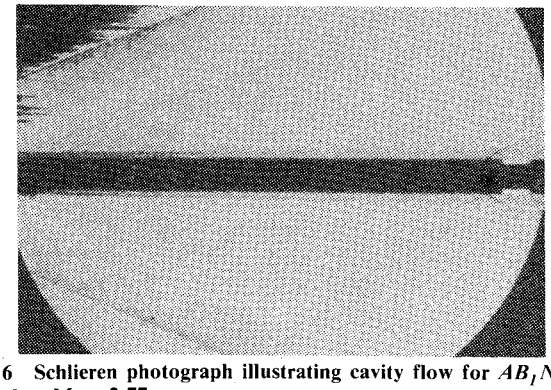

Fig. 6 Schlieren photograph illustrating cavity flow for AB_1N_1 at $\alpha = 0$ deg, $M_\infty = 2.77$.

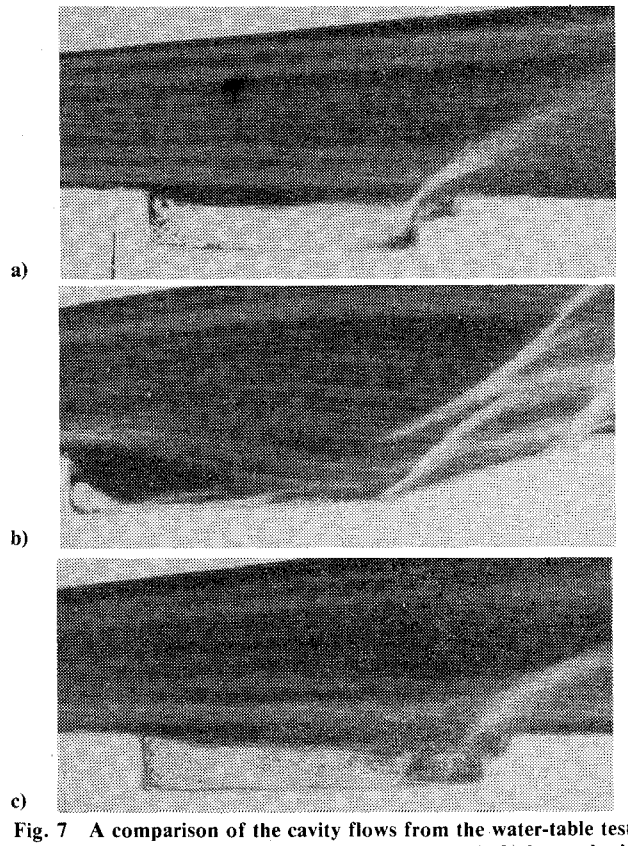

Fig. 7 A comparison of the cavity flows from the water-table tests, simulated $M_\infty = 2$: a) short cavity (original design), b) long, sloping cavity (closed flow), and c) "improved" long cavity design.

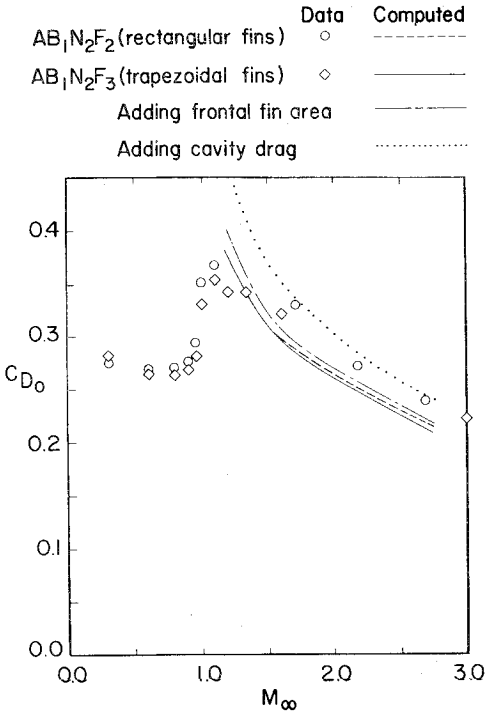

Fig. 8 Zero angle-of-attack drag coefficient for missiles with fins.

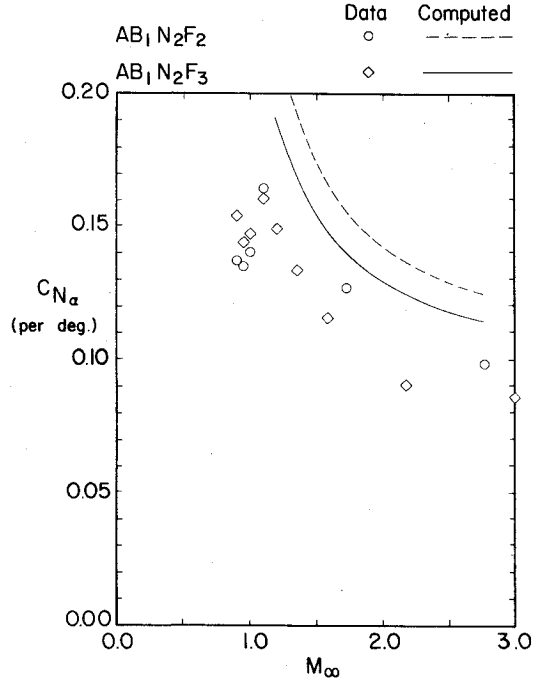

Fig. 9 Normal force coefficient derivative for missiles with fins.

fins. The values computed for the rectangular-fin configuration are slightly greater than those for the missile with the trapezoidal fin. The experimental values were also slightly greater for the rectangular-fin configuration.

The experimentally determined values of C_{N_α} for the two configurations are compared in Fig. 9 with the computed values. Experimental values are presented for Mach numbers from 0.9 to 3.03. Theoretical values are presented for Mach numbers of 1.2 or greater. The corresponding comparison for the center-of-pressure location is presented in Fig. 10. The normal-force coefficients and the pitching-moment coefficients are computed using planar-fin relations and the projected planform of the fins. Correlations presented in the

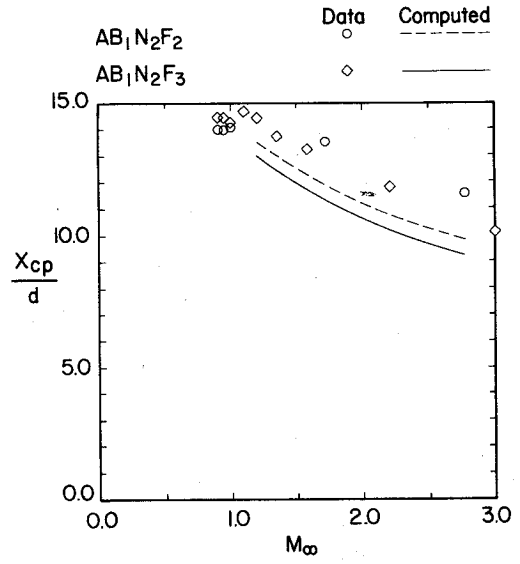

Fig. 10 Center-of-pressure locations for missiles with fins.

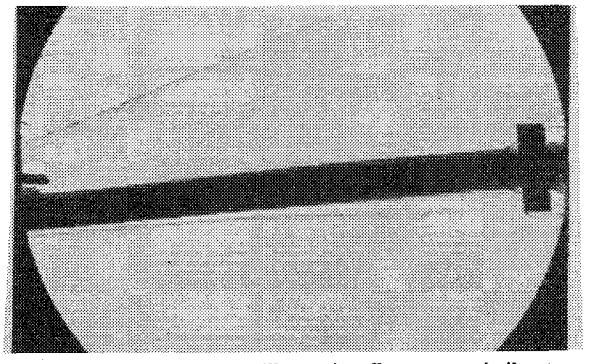

Fig. 11 Schlieren photograph illustrating flow over missile at $\alpha = 5$ deg, $M_\infty = 2.77$.

literature[1,6] indicate that the basic lifting characteristics of wrap-around fins are essentially the same as those for flat fins at angles of attack less than 6 deg.

The experimental values of C_{N_α} are typically 78% of the computed values for these supersonic flows. However, the experimentally determined center-of-pressure locations are further aft than the computed locations. The differences between experiment and computation are believed to be the result of viscous effects that are not incorporated into the computer flow model. Recall that the boundary layer for this long, slender missile is relatively thick, as can be seen by referring to the schlieren photograph of the body at zero angle of attack that is presented in Fig. 6. A schlieren photograph of the missile with rectangular fins ($AB_1N_2F_2$) at $\alpha = 5$ deg in a Mach 2.77 stream is presented in Fig. 11. The trace of the edge of the viscous region breaks away from the lee side of the missile at $x > 11d$. This suggests the presence of a free vortex layer type of separation.[18] The assumed flowfield contains helical (body) vortices with the separation of the circumferential flow component. These body vortices generate vortex lift in the aft region, moving x_{cp} aft. The flow still maintains a strong axial component. The presence of shock waves originating at the ramp and from the fin surfaces in the leeward region support the concept of a strong axial flow in this region. Note that Oberkampf and Bartel[19] state that the separation pattern is affected by long body lengths as well as angle of attack. Recall that the wind-tunnel model was approximately 19-calibers long. Thus, the body vortices exist even though the angle of attack is relatively low, i.e., 5 deg.

The fact that the experimentally determined locations of x_{cp} are further aft than the computed locations whereas the ex-

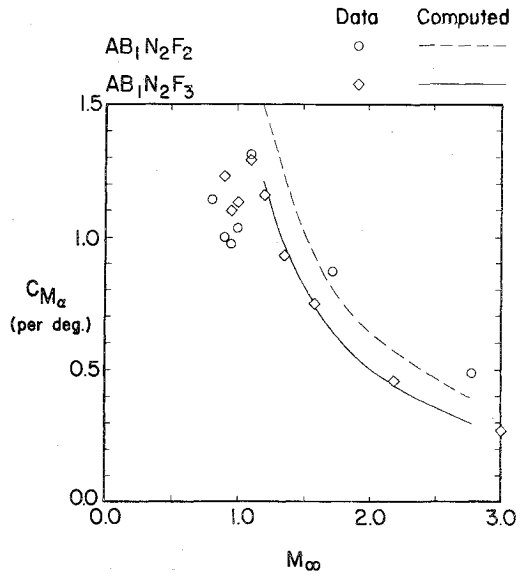

Fig. 12 Pitching moment coefficient derivative for missiles with fins.

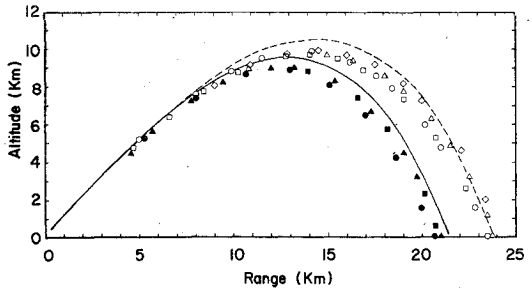

Fig. 13 A comparison of trajectories (from seven flight tests) for rockets with short motors, elevation of 48 deg, and short trapezoidal fins (open symbols represent data, --- computed) or long rectangular fins with a long "closed" cavity (closed symbols represent data, —— computed).

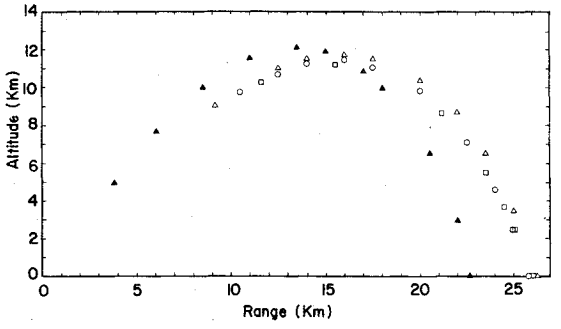

Fig. 14 A comparison of trajectories (from three flight tests) for rockets with long motors and long rectangular fins (filled symbols represent long "closed" cavity, 55 deg elevation; open symbols represent long "open" cavity, 50 deg elevation).

perimental values of C_{N_α} are less than the computed values suggests that the fins are not a dominant contributor to the discrepancy. Note that the computed contribution of the missile-body alone to C_{N_α} is roughly constant over the Mach number range. The fraction of C_N due to the body alone increases with Mach number until it is more than one-half when the Mach number is 2.18. Because the experimentally determined center of pressure is further aft than predicted, whereas the measured normal force is less than the computed value, discrepancies between the computed body force and the actual value are believed to be the principal source of the differences apparent in Figs. 9 and 10.

The measured values of C_{M_α} with respect to the center of gravity ($x_{cg} = 6.667d$) are compared with the computed values in Fig. 12. Note that the differences between experiment and computation for C_{N_α} and for x_{cp}/d compensate each other. As a result, the experimental values of C_{M_α} and the computed values are in excellent agreement.

The comparisons presented in this section clearly indicate that the computed aerodynamic coefficients are in reasonable agreement with the wind-tunnel measurements and with the water-table results. Furthermore, for the configurations tested, there was relatively little difference between the aerodynamic drag for missiles with rectangular fins and that for missiles with trapezoidal fins. The presence of the cavity housing the wrap-around fins did have a significant effect on the missile performance.

Having established that the computed aerodynamic coefficients are of engineering accuracy for these configurations, the computer code was used to generate the aerodynamic coefficients for the flight configurations. These coefficients were then used as input for a numerical routine to calculate the trajectories of the missiles.

Flight-Test Results

In conducting the initial design study for the 122-mm field-rocket system, the performance of trapezoidal fins was compared with that of rectangular fins. If the rocket flies at relatively high supersonic speeds and if the aerodynamic stability is marginal, rectangular fins are preferable. A negative consequence of using rectangular fins is increased drag at transonic speeds. Since this rocket flies at transonic speeds for most of the ballistic trajectory and since there was a sufficient margin of stability for the initial design, a trapezoidal planform was originally selected for the fins, see Fig. 4a. Trajectories from the flight tests of the initial design are presented as the open symbols of Fig. 13.

Due to new operational requirements, the motor length had to be increased. Rectangular fins of increased chord were chosen for the modified configuration. Since the size of the housing machined in the nozzle profile is related to the overall fin dimensions, the cavity length was increased to accommodate the longer fins. The initial design for the cavity housing these long rectangular fins is shown in Figs. 3b and 4b. Recall that the water-table tests indicate that the cavity flow is closed for this design. Trajectories for a missile with a short motor but with the long rectangular fins and the long "closed" cavity are presented as the filled symbols of Fig. 13.

Included for comparison are the trajectories computed at the University of Texas at Austin for the two configurations. Since the fin planform had a relatively small effect on the drag coefficients, the principal difference in the input values of the aerodynamic drag coefficients is due to the differences in the cavity geometry. The differences between the computed trajectories and the actual flight trajectories are attributed to minor differences between the assumed thrust history and the actual thrust history and between the estimated values and the actual values for the transonic drag of the missile. Nevertheless, both the computed trajectories and those obtained from the flight tests indicate that the configuration with the relatively long, "closed" cavity has a significantly shorter range. The significance of cavity drag is thus demonstrated by the wind-tunnel measurements, by the water-table results, and by the flight trajectories.

Using the results of the model studies discussed earlier in this paper, the cavity was redesigned. That is, the cavity was shortened so that it would have "open" flow but remained sufficiently long to house the long rectangular fins. The resultant L/H ratio was approximately 7.2, see Figs. 3c and 4c. The flight trajectories for two missile configurations with a long nozzle that housed long rectangular fins are compared in Fig. 14. (Note that there were differences in the initial elevation angle, as indicated in the legend.) The range of the missiles with long "closed" cavities is significantly less than

that of the missiles with long "open" cavities. Again, the cavity design has a significant effect on the range. However, it is clear that one can design a cavity that can house relatively long rectangular fins for a long motor configuration without sacrificing range. To do this, the cavity design should be such that the cavity flow is open.

Concluding Remarks

Data from wind-tunnel tests, water-table tests, and flight tests are presented for a long slender rocket with wrap-around fins. These data are compared with computed solutions obtained using state-of-the-art design codes. Based on the configurations and conditions considered in this investigation, the following conclusions are made.

1) There is reasonable agreement between the computed values and the wind-tunnel values of the aerodynamic coefficients. Using the projected (flat) planform area of the fins provides a reasonable estimate of the normal force produced by the wrap-around fins. The fact that the measured normal forces were below theory while the experimental locations of the center of pressure were further aft than the computed locations indicates that significant vortex lift was generated by body vortices.

2) The experimental results from all three test programs and the computed aerodynamic coefficients indicate that the drag produced by a closed cavity flow is considerably greater than that produced by an open cavity flow. The increased drag had a significant effect on the missile range. By carefully designing the cavity configuration, one can obtain both an open cavity flow for reduced drag and sufficient fin area for aerodynamic stability.

Acknowledgments

The authors are indebted to Janet Brooks and Liz Rich for their help in preparing the paper.

References

[1] Regan, F.J. and Schermerhorn, V.L., "Supersonic Magnus Measurements of the 10 Caliber Army-Navy Spinner Projectile with Wrap-Around Fins," U.S. Naval Ordnance Lab., NOLTR-70-211, Oct. 1970.

[2] Butler, R.W., "Evaluation of the Pressure Distribution on the Fins of a Wraparound Fin Model at Subsonic and Transonic Mach Numbers," Arnold Engineering Development Center, AEDC-TR-71-273, Dec. 1971.

[3] Dahlke, C.W. and Craft, J.C., "Aerodynamic Characteristics of Wraparound Fins Mounted on Bodies of Revolution and Their Influence on the Missile Static Stability at Mach Numbers from 0.3 to 1.3," U.S. Army Missile Command, RD-TM-72-1, March 1972.

[4] Holmes, J.E., "Wrap-Around-Fin (WAF) Pressure Distribution," U.S. Naval Ordnance Lab., NOLTR 73-107, Oct. 1973.

[5] Dahlke, C.W. and Flowers, L.D., "The Aerodynamic Characteristics of Wrap-Around Fins Including Fold Angle at Mach Numbers from 0.5 to 3.0," U.S. Army Missile Command, Tech. Rept. RD-75-15, Nov. 1974.

[6] Dahlke, C.W., "The Aerodynamic Characteristics of Wrap-Around Fins at Mach Numbers of 0.3 to 3.0," U.S. Army Missile Command, Tech. Rept. RD-77-4, Oct. 1976.

[7] Fournier, R.H., "Supersonic Aerodynamic Characteristics of a Series of Wrap-Around-Fin Missile Configurations," NASA TM-X-3461, March 1977.

[8] Swayer, W., Monta, W., Carter, W., and Alexander, W., "Control Characteristics for Wrap Around Fins on Cruise Missile Configurations," AIAA-81-0009, AIAA 19th Aerospace Sciences Meeting, St. Louis, Mo., Jan. 1981.

[9] Cantani, U., "Prove in Galleria Aerodinamica su Modelli dei Razzi da 50 mm e 120 mm (Gennaio-Febbraio 1978), Parte I: Descrizione e Raccolta dei Risultati," Difesa e Spazio, Colleferro, Italy, RE GAE 11.02, March 1978.

[10] DeAmicis, R. and Masullo, S., "Analisi Aerodinamica della Cavita' di Alloggiamento-Alette nel FIROS-25," Difesa e Spazio, Colleferro, Italy, NT GSR 11.48, Oct. 1980.

[11] Moore, F.G. and Swanson, R.C. Jr., "Aerodynamics of Tactical Weapons to Mach Number 3 and Angle of Attack 15°, Part I-Theory and Application," Naval Surface Weapons Center, NSWC/DL TR-3584, Feb. 1977.

[12] Swanson, R.C. Jr. and Moore, F.G., "Aerodynamics of Tactical Weapons to Mach Number 3 and Angle of Attack 15°, Part II-Computer Program and Usage," Naval Surface Weapons Center, NSWC/DL TR-3600, March 1977.

[13] Hoerner, S.F., *Fluid-Dynamic Drag*, published by the author, 1958.

[14] "Design for Control of Projectile Flight Characteristics," Engineering Design Handbook of the U.S. Army Material Command, AMCP 706-242, Sept. 1966.

[15] Charwat, A.F., Roos, J.N., Dewey, C.F. Jr., and Hitz, J.A., "An Investigation of Separated Flows-Part I: The Pressure Field," *Journal of the Aerospace Sciences*, Vol. 28, June 1961, pp. 457-470.

[16] Voorhees, C.G. and Bertin, J.J., "The Effect of Simulated Upstream Ablation on the Pressures in a Cavity," The University of Texas at Austin, Aerospace Engineering Rept. 68001, March 1968.

[17] Bouslog, S.A., "Computation and Analysis of Six-Degree-of-Freedom Trajectories," Presented at 26th Student Paper Competition, Southwest Region, April 1981.

[18] Stetson, K.F., "Experimental Results of Laminar Boundary Layer Separation on a Slender Cone at Angle of Attack at $M_\infty = 14.2$," Aerospace Research Labs., Wright-Patterson Air Force Base, Ohio, ARL 71-0127, Aug. 1971.

[19] Oberkampf, W.L. and Bartel, T.J., "Symmetric Body Vortex Wake Characteristics in Supersonic Flow," *AIAA Journal*, Vol. 18, Nov. 1980, pp. 1289-1297.